BRIEF RESEARCH COMMUNICATION

Potential Value of Fusion Imaging and Automated Three-Dimensional Heart Segmentation During Transcatheter Aortic Valve Replacement

Transcatheter aortic valve replacement (TAVR) has become the preferred procedure for aortic valve replacement.[1] Preprocedural multidetector computed tomographic (MDCT) imaging for aortic root analysis and prosthetic valve sizing is considered standard of care.[2] However, the use of iodinated contrast agent during MDCT angiography bears a significant nephrotoxicity risk in patients with chronic severe kidney failure. Three-dimensional (3D) transesophageal echocardiographic (TEE) imaging is considered a valuable alternative for aortic root sizing in this population.

Novel 3D TEE and fluoroscopic fusion software (FS) segments the heart and defines annular size completely user-independently. Furthermore, it allows live fusion of an anatomic heart model with fluoroscopy during structural heart interventions.[3] In this study, the safety and clinical benefit of this FS were assessed during TAVR.

We included 138 consecutive patients with severe aortic stenosis treated with TAVR. The first half (69 patients) was treated before the introduction of FS (FS− group), while periprocedural FS was used for the remaining 69 patients (FS+ group). The appropriate prosthesis size and type were chosen on the basis of clinical and anatomic criteria assessed by preprocedural MDCT imaging, not FS. TAVR was performed under general anaesthesia and 3D TEE guidance in all patients, as previously described by this group.[4] Eight patients had to be excluded from the study, because FS could not be used because of arrhythmias.

EchoNavigator release 3.0 (investigational device; Philips Medical Systems, Best, the Netherlands) was used in the FS+ group. On the basis of a 3D TEE volume (volume rate ≥ 15/sec; EPIQ 7C; Philips Medical Systems, Andover, MA) including the aortic root, both ventricles, and the complete mitral valve, the FS automatically generated an anatomic model with segmentation of all heart chambers, including the three aortic cusp nadirs, without the possibility of manual adjustments. To fuse the model with fluoroscopy, coregistration of the 3D TEE data set with fluoroscopy (Allura Xper FD20; Philips Medical Systems, Best, the Netherlands) in two different C-arm angulations is necessary (Supplemental Video 1, available at www.onlinejase.com). The anatomic model can then be used as electrocardiographically triggered overlay over fluoroscopy (Figure 1, Supplemental Video 2, available at www.onlinejase.com). In the FS− group, C-arm angulation during implantation was defined by preprocedural MDCT analysis and the use of contrast agent. In the FS+ group, the optimal C-arm position was found aligning the autogenerated cusp nadirs (Figure 2, Supplemental Video 3, available at www.onlinejase.com) instead of using MDCT values and contrast agent.

The FS-based anatomic model provided data on minimum, maximum, and mean annular diameter as well as annular perimeter and area (Figure 1). On the basis of these measurements, the potential prothesis size for each patient was reassessed. However, only MDCT sizing was used for implantation.

Most baseline characteristics and peri- and postinterventional outcomes did not differ significantly between the two groups (Supplemental Table 1). Procedure time was shorter in the FS+ group than in the FS− group (42.1 ± 15.2 vs 49.2 ± 20.7 min, respectively, $P = .024$), while contrast agent use (34.3 ± 22.0 vs 39.0 ± 23.3 mL, respectively, $P = .231$) and fluoroscopy time (11.4 ± 4.7 vs 10.9 ± 5.5 min, respectively, $P = .548$) did not differ.

FS-based annular measurements correlated well with MDCT measurements (Pearson correlation $r = 0.63–0.78$) but, with the exception of maximum diameter, were significantly larger than MDCT annular dimensions (Supplemental Table 2). However, the interacquisition variability for FS-based annular quantifications was very low (interclass correlation coefficient = 0.95–0.99). If valve sizing had been performed on the basis of FS measurements, the identical prosthetic valve size would have been chosen in 40 patients (61%), while 20 patients (30%) would have received larger and six patients (9%) smaller valve prostheses.

This is the first study analyzing the periprocedural use of novel FS during TAVR. Procedural characteristics and outcomes were similar for both groups, underlining the safety of the novel FS. The main procedural difference was the significantly shorter procedure time for FS+ patients. We assume that one of the main factors reducing procedure times was the very reliable, autogenerated aortic valve nadirs. Without FS, orienting the C-arm in the (MDCT imaging prespecified) optimal implantation angulation can be time and contrast agent consuming, as this may have to be repeated several times during TAVR. Furthermore, MDCT simulation of C-arm angulation chooses one position with equal distance between the nadirs. However, the annular plane can be found on multiple C-arm angulations, all of which can be used during implantation.[5] Using FS, the optimal C-arm angulation can be adjusted quickly and intuitively according to the patient's individual anatomy (i.e., obstructed views due to sternum cerclages or prosthetic material in mitral position). Because this was a rather small, nonrandomized study, selection bias cannot be ruled out as an additional factor contributing to the differences in procedure time.

In contrast to previous studies using FS during LAA closure,[6] our study did not reveal a significant reduction in contrast agent used. The use of FS-based aortic cusp nadirs did in our experience reduce the amount of contrast agent during C-arm optimization and the implantation itself. However, this effect was likely masked by the amount of contrast agent used to ensure absence of vascular

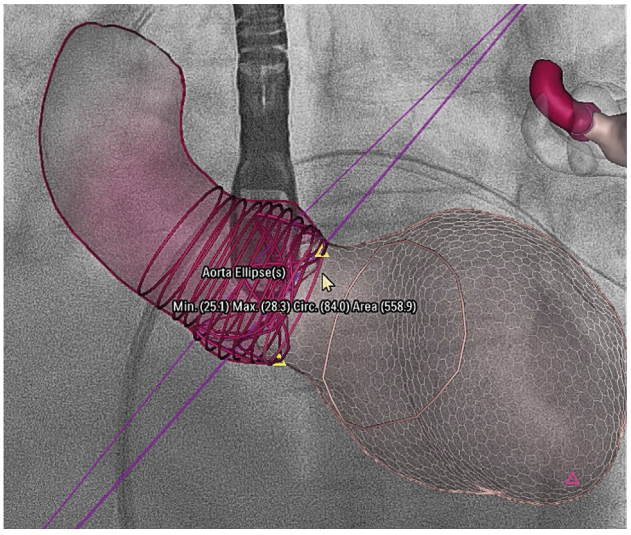

Figure 1 Three-dimensional model of aortic root and left ventricle overlaid with fluoroscopy. Fully automated measurements are displayed by selecting the respective structure, as shown here with the aortic annulus.

Drs. Biaggi and Sager contributed equally to this manuscript.

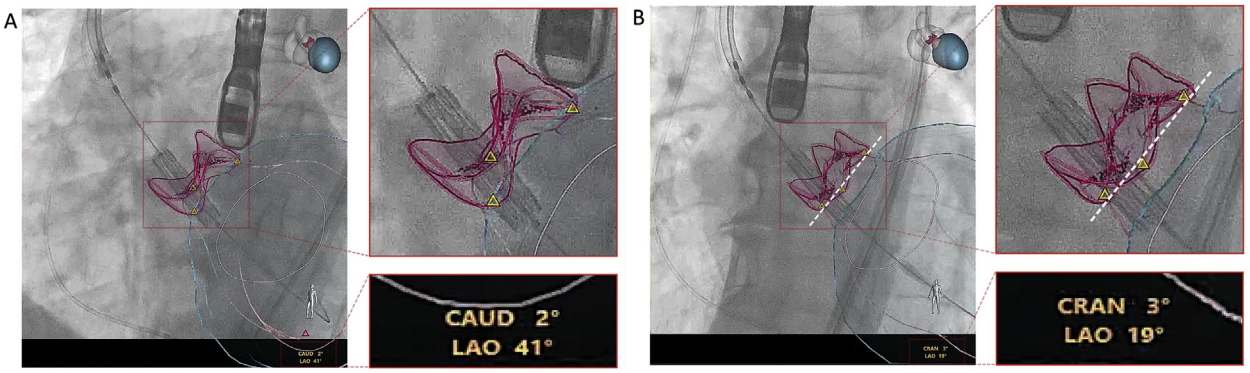

Figure 2 Using FS, the optimal C-arm angulation for prosthesis implantation can be found by direct visual control during C-arm rotation: **(A)** before and **(B)** after refinement of aortic annular plane alignment using aortic valve nadirs.

complications (mirrored by large SDs for overall small amounts of contrast agent).

FS-derived annular dimensions showed lower concordance with MDCT measurements compared with a similar study.[7] The present overestimation of annular dimensions by this FS is most likely due to an algorithm involving an elliptical approach (on the basis of maximum and minimum diameters) as opposed to a "true" anatomic analysis. To become a reliable sizing tool during TAVR, further refinements of the algorithm modeling the aortic root are necessary.

Many centers nowadays have switched to a minimalistic TAVR approach, without performing peri-interventional TEE imaging. However, the ongoing development of miniature 3D TEE probes that can be used under conscious sedation may allow the use of FS even in minimalistic TAVR. Assuming refinements leading to higher accuracy of the FS-derived annular dimensions, the rapid and user-independent annular measurements combined with automated cusp nadirs have the potential to become important tools for reliable "on-table" valve sizing and device implantation.

ACKNOWLEDGMENTS

We thank our study nurse, Verena Reichl, and the cardiac anesthetists for assisting us in collecting the data for this study.

SUPPLEMENTARY DATA

Supplementary data related to this article can be found at https://doi.org/10.1016/j.echo.2019.12.012.

Patric Biaggi, MD
Heart Clinic Zurich Hirslanden
Zurich, Switzerland

Dominik F. Sager, MBBS
Faculty of Medicine
University of Zurich
Zurich, Switzerland

Jeremy Külling, MSc
Department of Statistics
Swiss Federal Institute of Technology
Zurich, Switzerland

Silke Küest, MD
Christophe Wyss, MD
David Hürlimann, MD
Ivano Reho, MD
Ines Bühler
Georg Noll, MD
Heart Clinic Zurich Hirslanden
Zurich, Switzerland

Maurus Huber, MD
Heart Centre Hirslanden
Zurich, Switzerland

Oliver Gämperli, MD
Peter M. Wenaweser, MD
Roberto Corti, MD
Heart Clinic Zurich Hirslanden
Zurich, Switzerland

REFERENCES

1. Mack MJ, Leon MB, Thourani VH, Makkar R, Kodali SK, Russo M, et al. Transcatheter aortic-valve replacement with a balloon-expandable valve in low-risk patients. N Engl J Med 2019;380:1695-705.
2. Binder RK, Webb JG, Willson AB, Urena M, Hansson NC, Norgaard BL, et al. The impact of integration of a multidetector computed tomography annulus area sizing algorithm on outcomes of transcatheter aortic valve replacement: a prospective, multicenter, controlled trial. J Am Coll Cardiol 2013;62:431-8.
3. Biaggi P, Nijhof N, Corti R. Automated anatomical intelligence: next-generation fusion imaging during structural heart interventions. Eur Heart J 2017;38:1412.
4. Stahli BE, Bunzli R, Grunenfelder J, Buhler I, Felix C, Bettex D, et al. Transcatheter aortic valve implantation (TAVI) outcome according to standardized endpoint definitions by the Valve Academic Research Consortium (VARC). J Invasive Cardiol 2011;23:307-12.
5. Theriault-Lauzier P, Andalib A, Martucci G, Mylotte D, Cecere R, Lange R, et al. Fluoroscopic anatomy of left-sided heart structures for transcatheter interventions: insight from multislice computed tomography. JACC Cardiovasc Interv 2014;7:947-57.
6. Jungen C, Zeus T, Balzer J, Eickholt C, Petersen M, Kehmeier E, et al. Left atrial appendage closure guided by integrated echocardiography and fluoroscopy imaging reduces radiation exposure. PLoS One 2015;10:e0140386.

7. Prihadi EA, van Rosendael PJ, Vollema EM, Bax JJ, Delgado V, Ajmone Marsan N. Feasibility, accuracy, and reproducibility of aortic annular and root sizing for transcatheter aortic valve replacement using novel automated three-dimensional echocardiographic software: comparison with multi-detector row computed tomography. J Am Soc Echocardiogr 2018;31:505-5143.

https://doi.org/10.1016/j.echo.2019.12.012

Supplemental Table 1 Baseline characteristics and peri- and postprocedural results

	FS+ (*n* = 69)	FS− (*n* = 69)	*P*
Demographics			
Age, y	79.3 ± 8.8	83.1 ± 6.0	.003
Sex, female	41 (59.4)	46 (66.7)	.382
Clinical assessment			
Body surface area, m^2	1.8 ± 0.2	1.8 ± 0.2	.943
Systolic blood pressure, mm Hg	139.8 ± 21.1	139.3 ± 24.2	.898
Heart rate, beats/min	73.1 ± 13.7	74.9 ± 15.4	.464
Glomerular filtration rate, mL/min	64.7 ± 17.4	49.6 ± 21.9	<.001
EuroSCORE II, %	3.1 ± 2.8	4.0 ± 2.7	.054
Medical history			
Prior heart surgery	6 (8.7)	9.0 (13.0)	.416
Atrial fibrillation	15 (21.7)	19 (43.2)	.015
Peripheral artery disease	6 (8.7)	9 (13.0)	.416
Pacemaker	7 (10.3)	6 (8.7)	.752
Baseline echocardiography			
Left ventricular ejection fraction, %	59.8 ± 12.2	62.3 ± 15.2	.301
Left ventricular end-diastolic volume index, mL/m^2	54.5 ± 19.3	51.1 ± 16.6	.487
Left atrial volume index, mL/m^2	43.7 ± 15.3	53.6 ± 25.5	.069
Aortic valve area index, cm^2/m^2	0.5 ± 0.2	0.4 ± 0.1	.083
Mean gradient aortic valve, mm Hg	38.4 ± 17.6	43.8 ± 19.7	.117
Aortic valve regurgitation > 1*	9 (14.8)	5 (9.8)	.435
Peri-interventional data			
Interventional success	69 (100.0)	69 (100.0)	≥.999
Prosthesis type			
Edwards SAPIEN S3	37 (53.6)	39 (56.5)	.734
CoreValve R/Pro	22 (31.9)	13 (18.8)	.079
Symetis ACURATE neo	10 (14.5)	17 (24.6)	.135
Predischarge data			
In-hospital mortality	1 (1.4)	1 (1.4)	≥.999
Duration of stay, d	9.7 ± 5.9	9.7 ± 4.8	.992
Left ventricular ejection fraction, %	65.1 ± 9.2	65.0 ± 11.0	.945
Effective orifice area, cm^2	2.2 ± 0.8	2.2 ± 0.6	.763
Mean gradient aortic valve, mm Hg	8.2 ± 3.1	7.7 ± 3.5	.355
Aortic valve regurgitation > 1*	0 (0.0)	2 (3.3)	.147

EuroSCORE = European System for Cardiac Operative Risk Evaluation.
Data are expressed as mean ± SD or as number (percentage).
*Graded 0 = none or trace, 1 = mild, 2 = moderate, or 3 = severe.

Supplemental Table 2 Comparison of aortic annular dimensions by FS and MDCT imaging

Aortic annulus	FS	MDCT imaging	Mean difference	*P*
Area, mm^2	497.6 ± 106.7	440.2 ± 92.0	57.4 ± 66.9	<.001
Perimeter, mm	79.0 ± 8.4	75.5 ± 7.9	3.5 ± 5.6	<.001
Maximum diameter, mm	26.9 ± 2.8	26.8 ± 2.9	0.1 ± 2.4	.824
Minimum diameter, mm	23.3 ± 2.8	21.0 ± 2.5	2.3 ± 2.0	<.001
Mean diameter, mm	25.1 ± 2.7	23.9 ± 2.5	1.2 ± 1.8	<.001

Data are expressed as mean ± SD.